PERGAMON

Continental Shelf Research 22 (2002) 791–802

CONTINENTAL SHELF RESEARCH

www.elsevier.com/locate/csr

Upper ocean stratification and circulation in the northern Bay of Bengal during southwest monsoon of 1991

V.V. Gopalakrishna[a,*], V.S.N. Murty[a], D. Sengupta[b], Shrikant Shenoy[a], Nilesh Araligidad[a]

[a] *Physical Oceanography Division, National Institute of Oceanography, Dona Paula, Goa, 403 004, India*
[b] *Centre for Atmospheric and Oceanic Sciences, Indian Institute of Sciences, Bangalore, 560 012, India*

Received 3 March 2001; received in revised form 3 August 2001; accepted 28 August 2001

Abstract

During the southwest monsoon (July) of 1991 a large plume ($300 \times 250\,km^2$) of warm ($>29°C$) and less saline (<29 PSU) water is noticed in the top 30 m to the east of 87.5°E in the northern Bay of Bengal. To the west of 87.5°E, cold and saline waters are noticed in the upper 50 m, with a distinct thermo-haline front along 87.5°E. The thermohaline fields show the influence of wind forcing west and south of the front, but up to the base of the freshwater plume east of the front. Stable stratification and anticyclonic circulation associated with the freshwater plume restrict the entrainment of cold waters to the base of the stratified layer. In contrast, cyclonic circulation dominates in the plume area with reference to 500 db. The OGCM simulations driven by NCEP daily winds and COADS monthly winds for July 1991 agree well with the observations outside the plume area. The former simulation also identify a strong equatorward coastal current where there were no direct observations during the study period. The offshore location and thinning of the plume follow the Ekman dynamics in agreement with the numerical solutions of river plume (Continental Shelf Research 19 (1999) 1437, Journal of Geophysical Research 106 (C1) (2001) 1067).

Keywords: Bay of Bengal; Freshwater plume; Wind forcing; Thermohaline front; OGCM; Southwest monsoon

1. Introduction

The seasonal variation of hydrography and circulation of the Bay of Bengal has been reviewed recently by Varkey et al. (1996). Murty et al. (1992a) described the general hydrography and circulation of the waters of the Bay of Bengal during the southwest monsoon of 1984. These authors report the occurrence of lower (<20 PSU) sea surface salinity in the northern Bay due to precipitation and fresh water influx from the Brahmaputra and Ganges rivers. Gopalakrishna and Sastry (1985) reported intense downwelling along the west coast of the Bay at 18°N although the southwesterly winds were favorable for coastal upwelling. These authors argued that the equatorward flow of low salinity waters along the west coast of the Bay would over-compensate the waters replaced by the off-shore Ekman transport,

*Corresponding author. Tel.: +91-8322-26253; fax: +91-8322-23340.
E-mail address: gopal@darya.nio.org, gopal@csnio.ren.nic.in (V.V. Gopalakrishna).

0278-4343/02/$ - see front matter
PII: S0278-4343(01)00084-X

thereby suppresses the coastal upwelling. Babu et al. (1991) documented the presence of a cyclonic eddy off Visakhapatnam (18°N) during the southwest monsoon of 1984; the eddy was developed between the equatorward coastal current (carrying low salinity waters) and the offshore poleward current (wind driven). Shetye et al. (1991) reported the presence of a low salinity plume hugging the coast in the northwest Bay during July 1989.

The seasonal cycle of river runoff into the Bay attains a maximum during June–September/October, the southwest monsoon period and minimum during December–May (Han and McCreary, 2001). The influence of freshwater influx (through runoff and heavy precipitation over the Bay) complicates the hydrography and circulation of these waters. The contribution of local precipitation to the observed low salinity waters is yet to be quantified by satellite data analysis. In the present study, the authors discuss the hydrography and circulation of the waters in the northern Bay ($>16°$N) during southwest monsoon of 1991 and the observed circulation pattern is compared with the Ocean General Circulation Model (OGCM) simulations for the north Indian Ocean. Swathi et al. (2000) have simulated the Indian Ocean circulation using Hellerman and Rosenstein (1983) monthly climatological winds and Levitus (1982) temperature and salinity data. These authors have also done the simulations using COADS (Comprehensive Oceanic ans Atmospheric Data Sets) wind data set (at $2.5° \times 2.5°$ grid) for the study period (July 1991) and Levitus (1982) temperature and salinity data (Source: www.cmmacs.ernet.in\cgi_bin\climate_server\). Sengupta et al. (2001) carried out high resolution (at $0.33° \times 0.33°$ grid) simulations for the study period (July 1991) using the daily NCEP (National Center for Environmental Prediction) winds reanalysis (Kalnay, 1996) and Levitus and Boyer (1994) climatology. The results of these two simulations are shown in the present study.

2. Data and methods

A hydrographic survey was conducted in the northern Bay of Bengal (north of 16°N) during

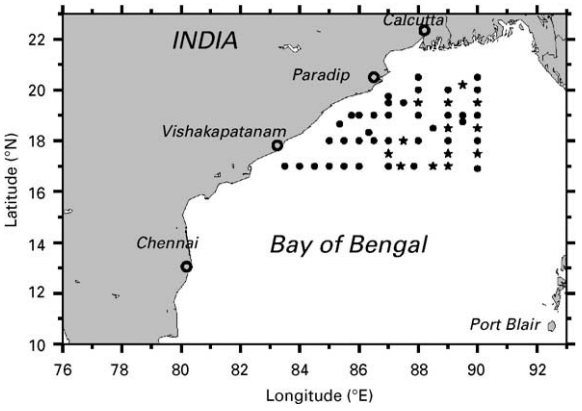

Fig. 1. Study area showing the network of hydrographic stations (full dot) and XBT stations (asterisk) in the northern Bay of Bengal.

11–24 July 1991 and 37 closely spaced (50–100 km apart) CTD stations and 14 XBT stations were occupied onboard O.R. V Sagar Kanya (Fig. 1). Temperature (T) and salinity (S) data were obtained using CTD system (M/s Sea Bird Electronics Inc., USA). At each CTD station water samples were collected through rosette samplers and analyzed for salinity using the AUTOSAL (Model 8400A, M/s Guildline, Canada). The AUTOSAL salinity values were utilized for correcting the CTD salinity. The Practical Salinity Scale (PSS-78) is used and salinity is mentioned in terms of PSU. The processed 1-m bin averaged temperature and salinity data were used to construct T and S profiles at each station and examined for spikes and spurious data. The data corresponding to the spikes were removed. Temperature vs. Salinity (T–S) plots were then prepared and the watermass structure is examined. In general, a wide scatter in the T–S plots is found in the upper 100 m, showing larger variability. Data points found as outliers were discarded. This quality controlled temperature and salinity data is used in the present analysis. Since our interest is to describe the upper ocean circulation and also considering the sampling depth at each station, we have chosen 500 db as the reference level to compute the dynamic heights and the geostrophic currents. The 3 h interval surface winds are used to compute the

zonal and meridional components of wind stress and Ekman transport.

3. Results and discussion

3.1. Hydrography

Figs. 2a and b show the distributions of sea surface temperature (SST) and sea surface salinity (SSS) in the northern Bay of Bengal during the southwest monsoon of 1991. The SST varied between 28.4°C and 29.5°C. A clear demarcation in the SST field is the occurrence of warmer waters (>29.0°C) to the east of 87.5°E and relatively cooler waters to its west. Similar demarcation is more evident in SSS field with intense lateral gradients separating the fresher waters (≪32.8 PSU) to the east of 87.5°E and north of 18°N and relatively saline waters (32.8–33.6 PSU) to its west. This observation clearly shows the presence of a thermohaline front oriented along 87.5°E between 18° and 21°N. The presence of such a thermohaline front in the open-northern Bay is not reported earlier. The boundary of the front is demarcated with the 29.0°C isotherm and 32.8 PSU isohaline

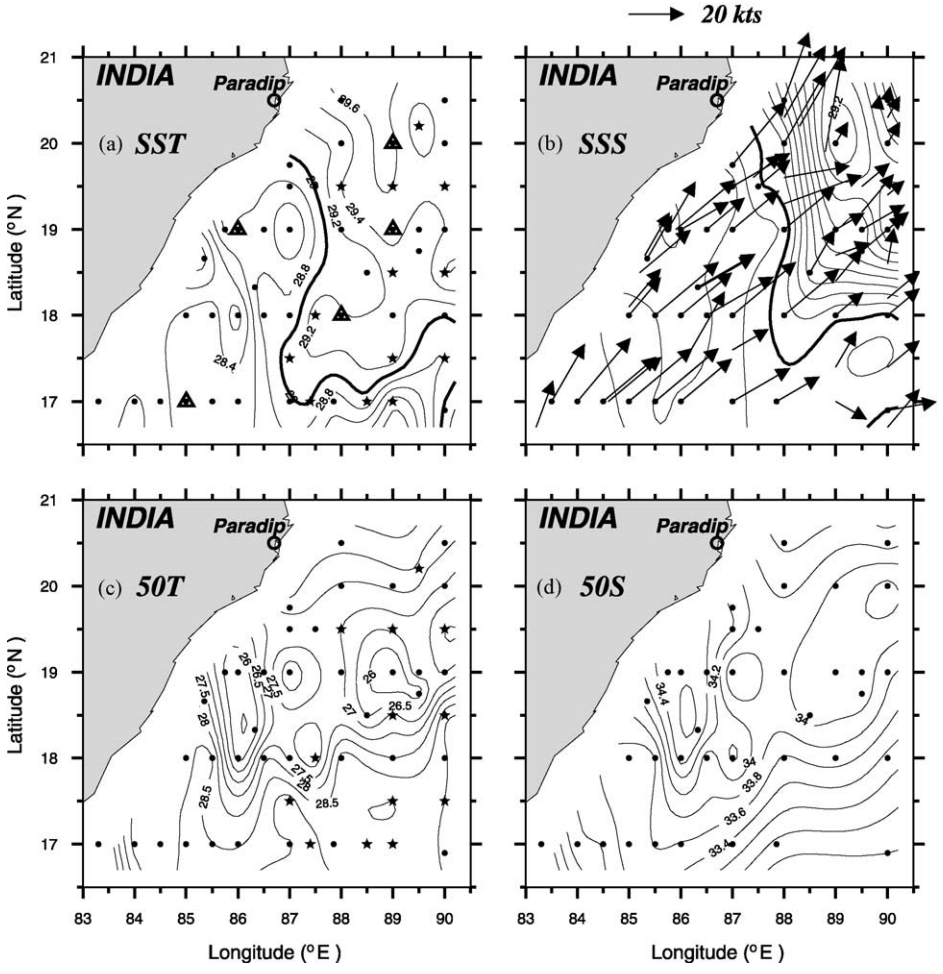

Fig. 2. Distribution of temperature and salinity (a,b) at sea surface and (c,d) at 50 m. Dots indicate CTD station locations. The thermohaline front is demarcated by thick isolines of 29°C and 32.0 PSU in (a,b). Stations inside the triangles correspond to Figs. 3 and 4. Wind vectors (arrows) are shown only at the hydrographic stations for clarity.

in Figs. 2a and b. The large cell of low saline waters ($\ll$32.8 PSU) to the east of 87.5°E is referred to as the freshwater plume and at the core of the plume the observed SSS is as low as 29 PSU. Thus, the freshwater plume is occupied over 0.8×10^5 km^2 area characterized with warm (29.0–29.5°C) and low saline (29.0–32.8 PSU) waters. Superimposed on SSS field is the observed surface winds showing strong south-westerlies west of 87.5°E and weaker southerlies to its east. The freshwater plume and the associated thermohaline front can be seen up to 30 m depth and disappears at 50 m depth (Figs. 2c and d). At this depth, warmer (28°C), less saline (32.8 PSU) waters occur south of the plume and colder (26°C), high saline (34.0–34.6 PSU) waters to the west of the plume and within it.

Typical profiles of temperature, salinity and density (sigma-*t*) are presented in Figs. 3a–d at 20°N, 89°E (within the plume), at 18°N, 88°E (southern extreme of the plume), and at 17°N, 85°E and 19°N, 86°E (outside the plume). These profiles show the nature of the homogeneous surface layer development. At the core of the plume, salinity rapidly increased by 3 PSU in the upper 25 m and slowly by 1 PSU between 25 and 50 m identifying the intense halocline (barrier layer) associated with the spread of low salinity

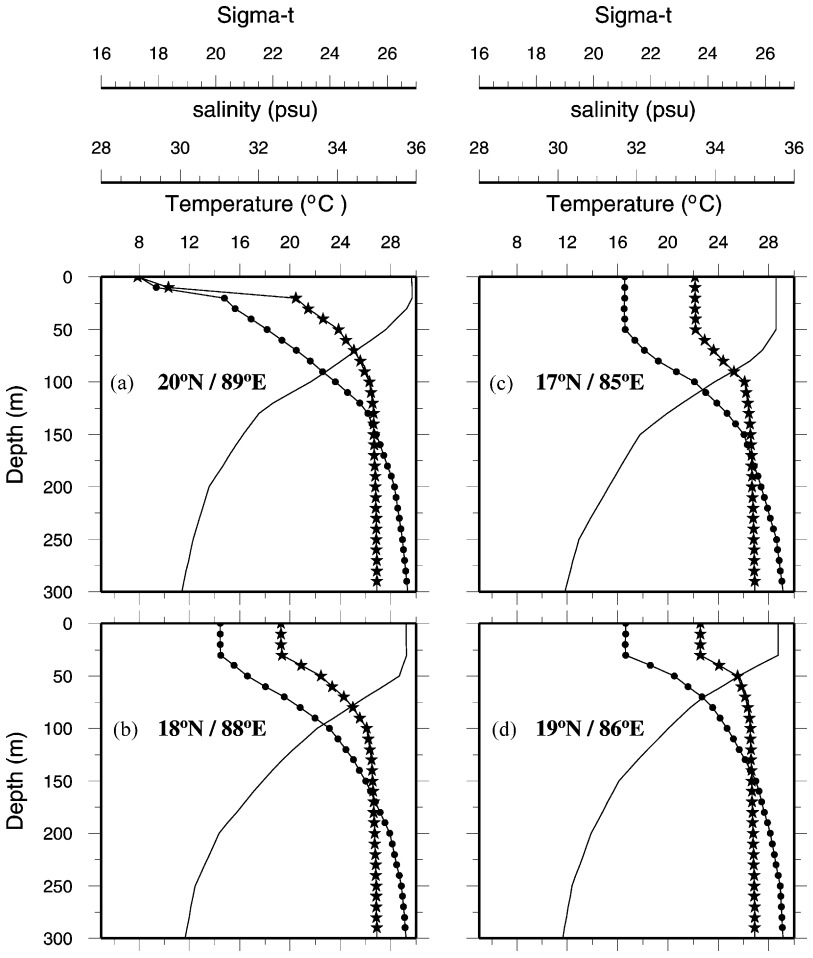

Fig. 3. Typical profiles of temperature (solid line), salinity (solid line with stars) and sigma-*t* (solid line with dots) at 4 selected locations marked (in Fig. 2a): (a) within the freshwater plume (20°N, 89°E), (b) southern extreme of the plume (18°N, 88°E) and (c,d) western side of the thermohaline front (17°N, 85°E; 19°N, 86°E).

waters. Apparently, there is no homogeneous (mixed) layer at the location within the plume (Fig. 3a). Similar observation is reported using the recently acquired CTD data in the northern Bay of Bengal during the southwest monsoon of 1999 under BOBMEX (Bay of Bengal Monsoon Experiment) (Vinayachandran et al., submitted for publication). As one moves away from the core of the plume, but along its axis, the mixed layer of 25 m thickness is seen clearly both in salinity and temperature (Fig. 3b). At 17°N, 85°E, the mixed layer is deep (50 m) in the case of temperature, but shallow (30 m) in the case of salinity and it is characterized by relatively cold and saline waters (Fig. 3c). However, at 19°N, 86°E the isothermal layer is shallower (25 m) than the isohaline layer (50 m) due to intense vertical mixing of upwelled cold-saline waters (Fig. 3d). At all the locations, the density in the mixed layer is controlled mainly by salinity changes than the changes in temperature—a characteristic feature of the Bay of Bengal during the southwest monsoon (Murty et al., 1992a, b, 1996).

Vertical sections of temperature and salinity along 90°E (Figs. 4a and b) clearly show the structure of the plume and its thermohaline characteristics. Intense halocline underneath the shallow homogeneous layer and deep homogeneous layer at the southern end of the plume followed by upslope of the isohalines from south to the base of the plume are evident. These structures indicate intense wind induced vertical mixing to the south of the plume, while this process (discussed below) limits entrainment of cold, saline waters up to the base of the halocline in the plume area.

The observed thermohaline fields contributed to a differential stratification regime in the study area. The degree of stratification is examined in terms of the static stability parameter (E) computed following Pond and Pickard (1983). The profiles of E are shown at five locations, that include the 4 locations where T and S profiles are presented (Fig. 3). The additional location is selected within the freshwater plume at 19°N, 89°E. At the core of the freshwater plume (20°N, 89°E), the profile of E shows a large stability maximum ($240 \times 10^{-5}\,m^{-1}$) at 25 m (Fig. 5a) coinciding with intense halocline. To the south of the core (19°N, 89°E), the stability maximum decreases and occurs at a deeper depth (Fig. 5a).

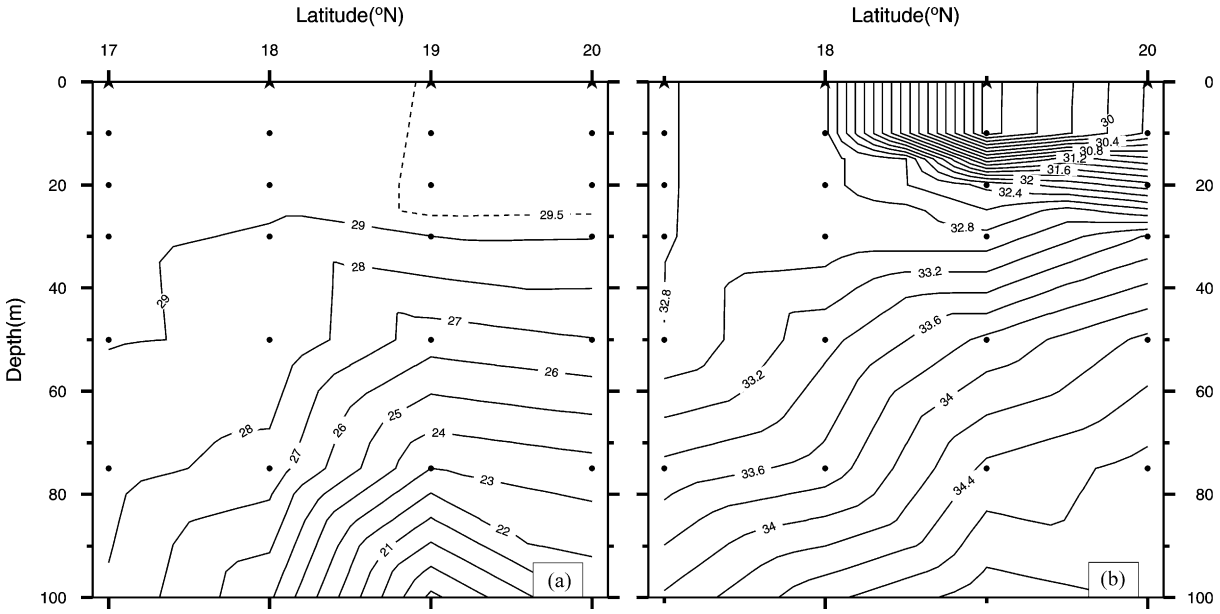

Fig. 4. Vertical sections of (a) temperature and (b) salinity along 90°E in the upper 100 m showing the thermohaline structures associated with the freshwater plume.

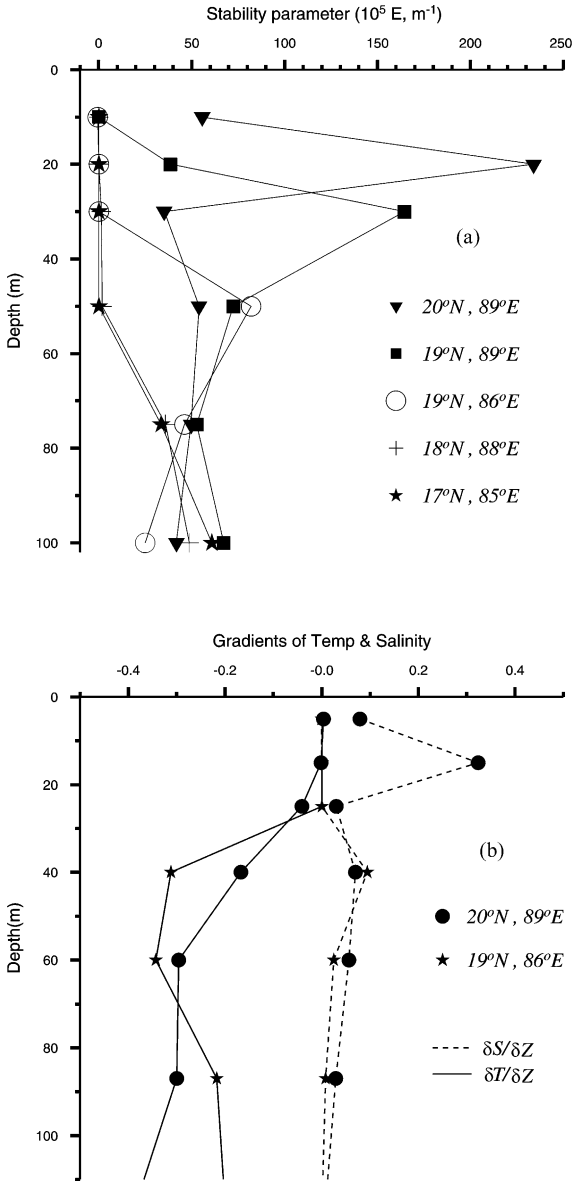

Fig. 5. (a) Typical profiles of Static Stability parameter (E) at the 5 selected locations (marked in Fig. 2a) and (b) typical profiles of vertical gradients of temperature and salinity in the upper 100 m at two locations (out of the 5 locations in Fig. 2a).

Towards the western edge of the plume (18°N, 88°E) and away from it (17°N, 85°E & 19°N, 86°E), weak to neutral stability conditions occur in the upper 50 m due to absence of near-surface low salinity waters. However, the weaker stability maximum at 50 m at 19°N, 86°E is due to the upwelling process (Fig. 3d). At all the locations, secondary stability maximum occurs at deeper depths corresponding to the thermocline. The profiles of vertical gradients of temperature (dt/dz) and salinity (ds/dz) in the upper 100 m are shown in Fig. 5b only at two locations—one at the core of the plume and the other outside the plume. These profiles highlight that the depth variation of stability parameter in the upper 50 m is affected more due to salinity gradients than the temperature.

3.2. Impact of the freshwater plume on the mixed layer depth and surface circulation

Murty et al. (1996) considered two criteria for the estimation of mixed layer depth (MLD), one is based on temperature and the other based on density considering (stratification). In the present study also, the two MLDs are estimated to understand the impact of the freshwater plume. The MLD defined as "*the depth where the water temperature is 1°C less to the SST (MLD-t)*" showed a plateau of smaller MLD-t (40 m) in the plume area (Fig. 6a). To the west and south of the front, the MLD-t deepens to 65–90 m. The distribution of MLD-σ_t, obtained as the "*depth where the vertical density gradient exceeds 0.02 Kg m^{-4} in the upper layers* (Vinayachandran et al., submitted for publication)" is similar to that of MLD-t. However, values of MLD-σ_t are reduced to $\sim$10 m in the plume area and to 35–60 m to the west and south of the front (Fig. 6b). These estimations of MLD-t and MLD-σ_t are in agreement with those reported by Murty et al. (1992a, b, 1996) for the northern Bay. The appreciable decrease by 25 m in the values of both MLD-t and MLD-σ_t in the plume area highlights the impact of low salinity waters on the MLD and its consequent effect (warm SSTs) on the air-sea interaction processes. The mean temperature in the upper 30 m is relatively larger in the plume area (28.9–29.5°C) which support organized deep convection over the northern Bay during the southwest monsoon. In fact, deep depression developed over the plume area at the end of the observational period.

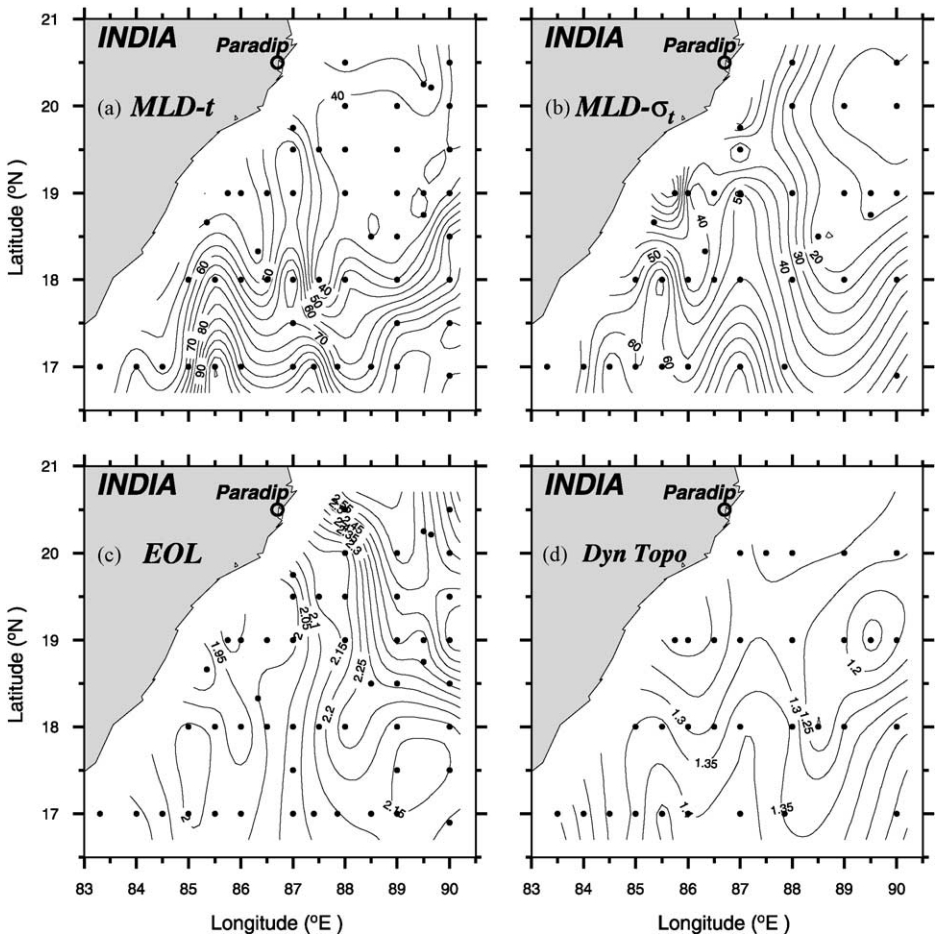

Fig. 6. Distribution of (a) temperature criterion based MLD-t (m) and (b) Sigma-t criterion based MLD-σ_t (m) and surface circulation based on (c) EOL parameter ($m^2 s^{-2}$) and (d) dynamic topography at sea surface relative to 500 dB.

Recently, while studying the impact of freshwater influx on the cyclogenesis over the Bay of Bengal, Murty et al. (2000) proposed a dynamic parameter "*the Effective Oceanic Layer (EOL)*". The EOL defined as the "*geopotential thickness of the near-surface stratified layer (surface to depth of stability maximum) formed due to spread of low salinity waters*" considers both temperature and salinity variations in the stratified layer. Since the EOL is a dynamic parameter with units of $m^2 s^{-2}$ (similar to dynamic height), its spatial distribution would represent the near-surface circulation without influenced by the interior thermocline processes. In order to understand the impact of freshwater plume on the near-surface circulation, we have compared the distribution of EOL (Fig. 6c) with the sea surface dynamic topography at sea surface (Fig. 6d) obtained by integration of geopotential anomaly from the reference level of 500 db. The plume area is characterised by higher values ($>2.2 m^2 s^{-2}$) of EOL and suggests anti-cyclonic (clockwise) circulation (with higher values to the right of the flow) between 87° and 90°E encompassing the plume. In the plume area, where the observed winds are weak, the MLD-σ_t is shallow and possesses higher EOL (warm and low salinity waters) and may play a dominant role on the air-sea coupling processes over the northern

Bay during the southwest monsoon. The anticyclonic flow associated with plume (Fig. 6c) is not seen in the sea surface dynamic height topography (Fig. 6d). It is to point out that the dynamic topography reflects largely the thermocline circulation due to large vertical gradients of temperature at subsurface depths, well below the lower depth limit of the freshwater plume (~ 30 m). This suggests that baroclinic current structure with considerable vertical shear is associated with the plume—an aspect yet to be established with direct current measurements. Outside the plume area, the dynamic topography shows a broad northerly flow with a surface velocity of 40–45 cm s^{-1} off the west coast of the Bay along 17°N and its turning towards east with undulations between 17° and 18.5°N. The transport of the northerly flow is about 8×10^6 m^3 s^{-1} in the upper 500 m. A mesoscale cyclonic eddy is centered at 19°N, 86°E outside the plume. An equatorward flowing coastal current is envisaged as a return flow of this eddy. In fact, the OGCM simulations (see Fig. 8) indicate a strong equatorward current along the west coast of the Bay (discussed in the next section). Thus the distributions of thermohaline fields, MLDs, EOL and sea surface dynamic topography highlight the impact of freshwater plume on the near-surface circulation during monsoon season in the northern Bay of Bengal.

3.3. *Influence of large-scale dynamics on the plume during the southwest monsoon*

The importance of surface wind stress and the associated Ekman transport on the movement of the freshwater plume in the Bay of Bengal is addressed recently Vinayachandran et al. (submitted for publication). In the present study, we have examined the distributions of both the zonal (τ_x) and meridional (τ_y) wind stress components and the associated Ekman transport (not shown here), computed using the 3-h wind data. These distributions indicate that the meridional wind stress component (positive, northward) and the associated zonal component of Ekman transport (positive, eastward) increase off-shoreward from the west coast of the Bay and attain larger positive magnitudes in a SW–NE band extending from the southwestern corner to the plume area. The offshore Ekman transport appears to be responsible for keeping the freshwater plume in the open-sea. The numerical model simulations of Xing and Davies (1999) and Fong and Geyer (2001) well support the above findings of this study, as the observed winds (in our study) are upwelling favourable and tidal influence is insignificant in the open-sea. It is interesting to note that these simulations suggest that mixing associated with the plume would be responsible for destroying the plume as it is advected far offshore (>40 km) from the coast (say, beyond 72 h). However, the present study shows that the plume is located well away from the coast (~ 200 km distance) with central low salinity waters of 29 PSU. It appears that the plume is maintained due to local precipitation without being destroyed by strong southwest monsoon winds. The drop in the salinity of the plume due to precipitation might counter the mixing processes. It is not certain to say whether the plume has been advected from the west coast of the Bay in the present study. It is worth mentioning that Shetye et al. (1991) reported the presence of freshwater plume (with central salinity <29 PSU) adjacent to coast between 16°N and 20°N in the northwestern Bay during southwest monsoon of 1989.

The earliest wind driven surface circulation studies of Varadachari and Sharma (1966) show eastward flow during July–August in the northern Bay highlighting the possibility of eastward advection of surface waters. The field of wind stress curl (WSC) computed using the daily NCEP winds for the study period (11–24 July 1991) shows upwelling-favourable positive WSC in the northern Bay (Fig. 7a) with larger magnitude ($>4 \times 10^{-7}$ N m^{-3}) west of 87°E and weaker magnitude ($<3 \times 10^{-7}$ N m^{-3}) over the plume area. The observed cooler, saline and homogeneous and deeper MLDs west of 87°E strongly support the process of wind-induced-upwelling and the associated intense vertical mixing (Fig. 3d, for example). The influence of wind forcing in the plume area can only be seen below the depth of the stratified layer as seen from the thermohaline fields (Figs. 2c, 4a and b). Consequently, entrainment of cold, saline waters towards the surface is confined

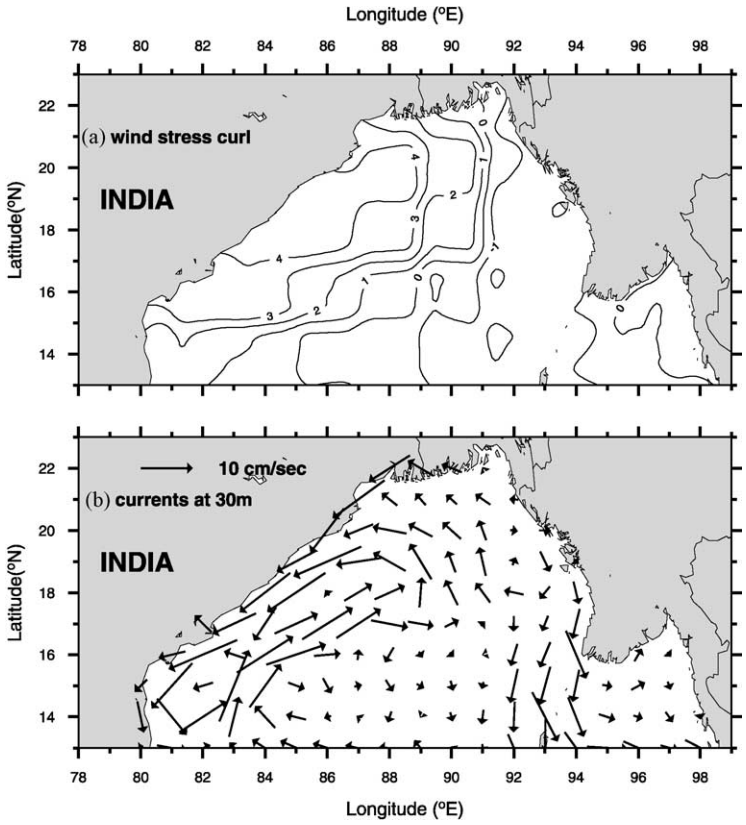

Fig. 7. (a) Distribution of wind stress curl ($\times 10^{-7}\,\mathrm{Nm}^{-3}$) computed using daily NCEP winds for the study period and (b) Modular Ocean Model version 2 (MOM-2) OGCM simulated currents at 30 m for July 1991 driven by daily NCEP winds. The surface temperature and salinity values are restricted to those of climatological values (Levitus and Boyer, 1994). The currents are shown at the center of the grids ($0.33^\circ \times 0.33^\circ$)

up to the depth of stability maximum ($\sim$30 m). Similar observation was reported earlier by Murty et al. (1996) at a stationary location (20°N, 89°E) in the northern Bay during August–September 1990. As upwelling process is weakened in the stratified plume, a weaker cyclonic circulation is resulted in the plume area (Fig. 5d).

3.3.1. Comparison of observed circulation with model simulations

In this section we present the results of OGCM numerical simulations of horizontal currents in the upper layer. More descriptions of the model setup may be found in Swati et al. (2000) and Sengupta et al. (2001) for each of the simulation studies. These models do not include freshwater influx or rain. Surface temperature and salinity are restricted to climatological temperature and salinity at the surface (Levitus, 1982; Levitus and Boyer, 1994). The model output of Swathi et al. (2000) begins from 5 m level while that of Sengupta et al. (2001) begins only from 30 m, the approximate lower limit of near-surface stratified layer. So, comparison of the observed circulation with Sengupta et al. (2001) is possible only outside the plume area and at 30 m depth and below. The model currents at 30 m depth for July 1991 are shown in (Fig. 7b). The wind forcing in Fig. 7a drives an elongated (with SW–NE orientation) cyclonic gyre in the northwestern Bay (Fig. 7b). A strong (30–60 cm s^{-1}) equatorward coastal current and an offshore northeastward flow across 16°N

extending up to the plume area constitute the cyclonic gyre. A part of the northeastward flow meanders towards the open sea between 16° and 17°N. These model currents outside the plume area coincide well with the observed flow field (Fig. 5d). The numerical simulations of Han et al. (2001) also point out the existence of an equatorward coastal current due to Kelvin waves generated under the influence of run-off from Ganges–Brahmaputra river system. The existence of this coastal current can also be envisaged as a return flow of the observed cyclonic circulation west of 87°E (Fig. 5d). The model results, however, do not depict the anticyclonic circulation associated with the freshwater plume (as inferred from the EOL distribution). The model results of Swathi et al. (2000), however show eastward currents at 5 m depth (Fig. 8a) and westward currents at 25 m (Fig. 8b) in the study area. The two model results show a good comparison at 30 and 25 m depth with a general westward flow north of 18°N. Moreover, the eastward currents at 5 m and westward currents at 25 m (Fig. 8a and b) do suggest the presence of baroclinic current structure (strong current shear) in the plume area. The numerical simulations of the river plume (Xing and Davies, 1999; Fong and Geyer, 2001) also indicate current shear with offshore flow at the surface and onshore flow below the base of the plume. The above plume simulation studies also show anticyclonic (clockwise) flows around the plume with less salinity waters at its center and

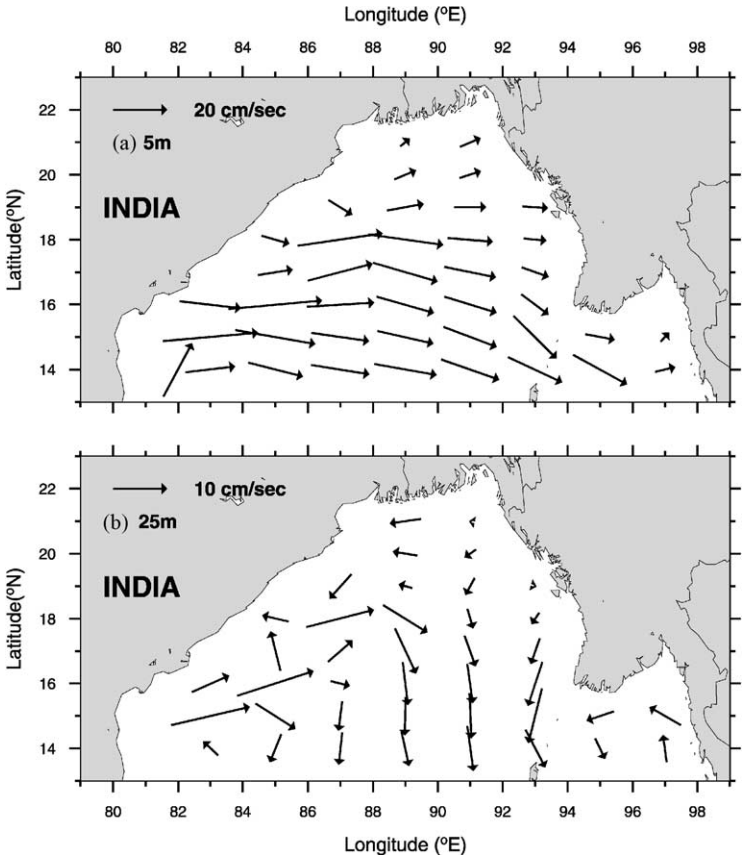

Fig. 8. (a) Modular Ocean Model version 2 (MOM-2) OGCM simulated currents at (a) 5 m and (b) 25 m depths driven by COADS wind data for July 1991 and Levitus (1982) temperature and salinity data. Surface temperature and salinity values are restricted to those of climatological values (Levitus, 1982). The current vectors are shown at the center of the grids ($2.5^\circ \times 2.5^\circ$).

supports the observed flow pattern as inferred from EOL distribution (Fig. 5c). The discrepancy between the OGCM simulated currents and observed currents in the plume area highlights that one should include the freshwater influx or rain in the model for a complete description of near-surface flow field in the Bay of Bengal. The recent model studies by Han and McCreary (2001) consider various causes for modeling the salinity distribution in the Indian Ocean in different layers without wind forcing. The model solutions pertaining to Precipitation minus Evaporation and the run-off from Ganges–Brahmaputra river system (their Plate 3a) in the layer 1 do agree with the observed salinity distribution and the model current vectors are directed eastward in the present study area. We feel that if the model's upper layer in Han and McCreary (2001) is restricted to the stratified layer ($\sim$upper 30 m), then reliable circulation patterns would be expected, as that of EOL to understand the near-surface circulation in the Bay of Bengal.

4. Summary

CTD data collected from a net work of stations in the northern Bay during southwest monsoon of 1991 yielded demarcation of a plume of warm, less saline waters in the open sea, separated by a thermohaline front along 87.5°E from the cold, saline waters. The influence of wind forcing (positive WSC) is more evident to the west of the thermohaline front, while it is limited up to the base of the near-surface stratified layer in the plume area. It is seen that the zonal component of Ekman transport and model currents at 5 m (Swathi et al., 2000) keep the plume away from the west coast of the Bay. The geostrophic circulation outside the plume area is well reproduced in the OGCM simulations driven by NCEP daily winds for July 1991. On the other hand, it is revealed that the EOL parameter is useful to describe the near-surface layer circulation in the region influenced by low salinity waters (plume area). The simulated currents show the existence of a strong equatorward coastal current off the west coast of the Bay.

Acknowledgements

This work is carried out under the Ocean Observing System (OOS) project funded by Department of Ocean Development, New Delhi. The authors (SS and NA) are thankful to DOD for providing Project Assistantship. One of the results of MOM-2 OGCM simulations (u and v components of currents) are downloaded from the website managed by CMMACS, Bangalore (site given in the text). This is the NIO contribution No. 3698.

References

Babu, M.T., Prasanna Kumar, S., Rao, D.P., 1991. A subsurface cyclonic eddy in the Bay of Bengal. Journal of Marine Research 49, 403–410.

Fong, D.A., Geyer, W.R., 2001. Response of river plume during an upwelling favourable wind event. Journal of Geophysical Research 106 (C1), 1067–1084.

Gopalakrishna, V.V., Sastry, J.S., 1985. Surface circulation over the shelf off the east coast of India during the southwest monsoon. Indian Journal of Marine Sciences 14, 62–65.

Han, W., McCreary Jr., J.P., 2001. Modeling salinity distributions in the Indian Ocean. Journal of Geophysical Research 106 (C1), 859–877.

Han, W., McCreary Jr., J.P., Kohler, K.E., 2001. Influence of precipitation minus evaporation and Bay of Bengal rivers on dynamics, thermodynamics and mixed layer physics in the upper Indian Ocean. Journal of Geophysical Research 106 (C4), 6895–6916.

Hellerman, S., Rosenstein, M., 1983. Normal monthly stress over the world ocean with error estimates. Journal of Physical Oceanography 13, 1093–1104.

Kalnay, 1996. The NCEP/NCAR 40-year reanalysis project. Bulletin of American Meteorological Society 77, 437–471.

Levitus, S., 1982. Climatological Atlas of the World Ocean, NOAA Prof. Paper No. 13, US Government Printing Office, 173pp.

Levitus, S., Boyer, Y.P., 1994. World Ocean Atlas, 1994, Vol. 4, Temperature, NOAA Atlas NESDIS, 4 US Dept of Commerce, Washington, USA, 117pp.

Murty, V.S.N., Sarma, Y.V.B., Rao, D.P., Murty, C.S., 1992a. Water characteristics, mixing and circulation in the Bay of Bengal during southwest monsoon. Journal of Marine Research 40, 207–228.

Murty, V.S.N., Sarma, Y.V.B., Babu, M.T., Rao, D.P., 1992b. Hydrography and circulation in the northwestern Bay of Bengal during the retreat of southwest monsoon. Proceedings of the Indian Academy of Sciences, Earth and Planetary Sciences 101, 67–75.

Murty, V.S.N., Sarma, Y.V.B., Rao, D.P., 1996. Variability of the Oceanic boundary layer characteristics in the northern Bay of Bengal during MONTBLEX-90. Proceedings of the Indian Academy of Sciences, Earth and Planetary Sciences 105, 41–61.

Murty, V.S.N., Sarma, M.S.S., Tilvi, V., 2000. Seasonal cyclogenesis and the role of near-surface stratified layer in the Bay of Bengal. Proceedings of PORSEC 2000, Vol. I, pp. 453–457.

Pond, S., Pickard, G.L., 1983. Introductory Dynamic Oceanography, Pergamon Press, New York, 241pp.

Sengupta, D., Senan, R., Goswamy, B.N., 2001. Origin of intraseasonal variability of circulation in the tropical central Indian Ocean. Geophysical Research letters 28, 1267–1270.

Shetye, S.R., Shenoy, S.S.C., Gouveia, A.D., Michael, G.S., Sundar, D., Nampoothri, G., 1991. Wind driven coastal upwelling along the western boundary of the Bay of Bengal during the southwest monsoon. Continental Shelf Research 11, 1397–1408.

Swathi, P.S., Sharada, M.K., Yajnik, K.S., 2000. A coupled physical-biological-chemical model for the Indian Ocean. Proceedings of Indian Academy of Sciences (Earth and Planet Science) 109, 503–507.

Varadachari, V.V.R., Sharma, G.S., 1966. Circulation of the surface waters in the north Indian Ocean. Journal of Indian Geophysical Union 4, 61–74.

Varkey, M.J., Murty, V.S.N., Suryanarayana, A., 1996. Physical oceanography of the Bay of Bengal and Andaman Sea. Oceanography and Marine Biology (an annual Review) 34, 1–70.

Vinayachandran, P.N., Murty, V.S.N., Rameshbabu, A. Observations of the monsoon halocline in the northern Bay of Bengal. Journal of Geophysical Research, submitted for publication.

Xing, J., Davies, A.M., 1999. The effect of wind direction and mixing upon the spreading of a buoyant plume in a non-tidal regime. Continental Shelf Research 19, 1437–1483.